

Testing turbulence models to predict interzonal mass airflows through a stairwell opening for both natural and mixed convection flows in buildings

Evaluación de modelos de turbulencia para predecir los flujos de masa de aire interzonas a través de una abertura de escalera para la convección natural y mixta en los edificios

Sergio Vera^{1*}, Magdalena Cortés*, Jiwu Rao**, Paul Fazio^{†**}, Waldo Bustamante*

* Pontificia Universidad Católica de Chile, Santiago. CHILE

** Concordia University, Montreal. CANADA

Fecha de Recepción: 02/06/2015

Fecha de Aceptación: 21/07/2015

PAG 85-97

Abstract

The main objective in building design is to balance energy efficiency with healthy, comfortable and productive indoor environments for the occupants. Interior building openings, such as stairwells, are significant paths for the exchange of heat, air, moisture and pollutants. The interzonal airflow through horizontal openings has not been profoundly studied because of its highly transient and unstable nature, the complexity of carrying out experiments and the limited availability of experimental data. Computational Fluid Dynamics (CFD) is an excellent tool to advance the understanding of this phenomenon. In this paper, CFD is applied to evaluate the performance of five two-eddy viscosity turbulence models ($k-\epsilon$ standard, $k-\epsilon$ RNG, $k-\epsilon$ realizable, $k-\omega$ standard and $k-\omega$ SST) to predict indoor air conditions and upward mass airflows through a horizontal opening in a full-scale, two-story test hut. This study involves six cases with different temperature gradients between the two floors and with three ventilation strategies that represent natural or mixed convection. The main results show that the temperatures are well predicted by all turbulence models while the simulated air speeds present larger variations among the evaluated turbulence models. Overall, the $k-\epsilon$ standard and $k-\epsilon$ realizable models are the most accurate ones to predict indoor temperatures and air speeds for natural and mixed convection, respectively. Moreover, the upward mass airflows through the horizontal opening estimated by both turbulence models are in very good agreement with the experimental data.

Keywords: Vertical interzonal airflows; horizontal opening; two eddy-viscosity turbulence models; natural convection; mixed convection

Highlights:

- Five turbulence models are evaluated against experiments in a full scale two-story test-hut
- Indoor air conditions and vertical interzonal mass airflows are forecasted by CFD
- The $k-\epsilon$ and $k-\omega$ turbulence models predict the temperature distribution accurately
- The $k-\epsilon$ realizable model is the most accurate one to predict air speed distribution
- The $k-\epsilon$ standard and $k-\epsilon$ realizable models excellently predict the interzonal airflow

Resumen

El objetivo principal del diseño de edificios es el proveer ambientes interiores productivos, confortables y saludables para sus ocupantes en balance con la eficiencia energética. Aberturas interiores de edificios, tales como las de escaleras, son huellas importantes para el intercambio de calor, aire, humedad y contaminantes. Los flujos de aire interzonas a través de aberturas horizontales no han sido estudiados profundamente debido a su naturaleza transiente y altamente inestable, la complejidad para realizar experimentos, y la escasez de datos experimentales disponibles. La Dinámica de Fluidos Computacional (CFD por su acrónimo en inglés) es una excelente herramienta para avanzar en la comprensión de este fenómeno. En este artículo, se aplica CFD para evaluar el desempeño de cinco modelos de turbulencia de dos ecuaciones: $k-\epsilon$ estándar, $k-\epsilon$ RNG, $k-\epsilon$ realizable, $k-\omega$ estándar y $k-\omega$ SST, para predecir las condiciones del aire interior y los flujos de la masa de aire ascendente que fluyen a través de una abertura horizontal en una casa de ensayos de dos pisos a escala real. La investigación incluye seis casos con diferentes gradientes de temperatura entre los dos pisos y tres estrategias de ventilación que representan convección natural y mixta. Los principales resultados muestran que las temperaturas son predichas correctamente por todos los modelos de turbulencia, mientras que las velocidades del aire simuladas presentan variaciones mayores entre los modelos de turbulencia evaluados. En general, los modelos $k-\epsilon$ estándar y $k-\epsilon$ realizable son los más precisos para predecir las temperaturas interiores y las velocidades de aire para la convección natural y mixta, respectivamente. Además, los flujos de la masa de aire ascendente a través de la abertura horizontal estimados por ambos modelos de turbulencia concuerdan muy bien con los datos experimentales.

Palabras clave: Flujos de aire vertical interzonal, aberturas horizontales, modelos de turbulencia de dos ecuaciones, convección natural, convección mixta

Aspectos destacados:

- Se evaluaron cinco modelos de turbulencia contrastándolos con los experimentos realizadas en una casa de ensayo de dos pisos de escala real
- Se usó la técnica CFD para predecir las condiciones del aire interior y los flujos de las masas de aire vertical entre las zonas
- Los modelos de turbulencia $k-\epsilon$ y $k-\omega$ evaluados predijeron con precisión la distribución de la temperatura
- El modelo $k-\epsilon$ realizable es el más preciso para predecir la velocidad de intercambio de los flujos de aire
- Los modelos $k-\epsilon$ estándar y $k-\epsilon$ realizable se desempeñan en forma excelente para predecir los flujos de aire entre las zonas

1. Introduction

The staircases of multi-story houses and buildings are the main paths for the interzonal air, moisture, heat and

pollutant exchange between different floors. The heat and mass that are transported through stairwell openings could have significant effects on the building energy consumption, indoor air quality, ventilation effectiveness and the spread of fire and smoke during building fires. Despite the importance of heat and mass exchange through horizontal openings in buildings, there is very limited information on both natural convection (Brown, 1962; Epstein, 1988; Riffat and Kohal, 1994; Peppes et al., 2001;

¹ Corresponding author:

Assistant Professor Departamento de Ingeniería y Gestión de la Construcción,
Pontificia Universidad Católica de Chile
E-mail: svera@ing.puc.cl



Blomqvist and Sandberg, 2004; Heiselberg and Li, 2009) and mixed convection (Vera et al., 2010a; Vera et al., 2010b; Tan and Jaluria, 2001; Klobut and Sirén, 1994; Cooper, 1995). Most of these studies have been performed using small-scale experiments, and they used saline water (brine) instead of air. Full-scale experiments using air as the working fluid are expensive, time consuming and complex to carry out. For this reason, there have been some attempts to study this phenomenon by means of Computational Fluid Dynamics (CFD).

Few authors have used the CFD technique to study the airflow exchange through horizontal openings, and most of them have focused on buoyancy-driven flows. Riffat and Shao (1995) performed one of the first studies on natural convection flow through horizontal opening using a transient and two-dimensional CFD simulation. The CFD results revealed the highly transient flow patterns at the horizontal opening. The air exchange rate between the two zones was continuously oscillating and with intermittent pulses. The predicted air exchange rate between the two zones obtained via CFD showed good agreement, 10.5% relative difference with the experimental data of Riffat et al. (1994). However, this study does not provide information on the turbulence model that was used to solve the Navier-Stokes equations.

Peppes et al. (2001) presented the measurements and CFD modeling of the buoyancy-driven flows through a stairwell connecting two individual floors to study the mass and heat transfer between the floors. The airflow rate was measured using the tracer gas technique. They noted that the airflow rate between the two floors was determined by the size and geometry of the opening separating the floors and by the air temperature differences between the upper and lower floors. With their experimental data, the authors proposed empirical correlations between the mass and heat flow rate through the stairwell opening. These experimental cases were simulated using the CFD technique. The $k-\varepsilon$ RNG model was chosen because of its ability to predict both high and low Reynolds number flows. The relative differences between the CFD and the experimental results for the airflow rates through the opening remained below 11.6% for all experiments. In a subsequent study Peppes et al. (2002) extended their investigation to an experimental and numerical study of a three-story building. The same turbulence model was used, and the CFD and experimental data showed very good agreement.

Li (2007) also studied natural convection flows through square horizontal openings via CFD by modeling a three-dimensional test-room with an upper opening. These CFD simulations were time dependent, and two turbulence models were evaluated: the $k-\varepsilon$ standard and Large Eddy Simulation (LES). The LES model was able to capture the bidirectional flow observed experimentally and agrees well with the measurements. Otherwise, the $k-\varepsilon$ standard turbulence model demonstrated poor performance because the airflow rate through the opening was significantly underpredicted.

More recently, Vera et al. (2010a) performed a unique experiment on the interzonal air and moisture transport through a horizontal opening in a full-scale, two-story test hut dominated by mixed convection. The indoor air conditions across the test hut and the mass flow rates through the opening under different scenarios were measured experimentally. Vera et al. (2010b) extended

their experimental study by means of CFD simulations. These CFD simulations were performed using the indoor zero-equation turbulence model developed by Chen and Xu (1998). The CFD results verified that a two-way airflow existed even in cases with warmer upper room. The CFD model was extensively validated, and the CFD results agreed well with the experimental data with regards to air speed, temperature, humidity ratio and interzonal mass airflows. Based on the same CFD simulation data of Vera et al. (2010b), Vera et al. (2014) established a correlation that represents the mixed convective heat transfer through the horizontal openings.

The above review shows the scarcity of studies on evaluating turbulence models to predict, first, the indoor air conditions in rooms connected by a horizontal opening and, second, the heat and mass exchange through these openings. In contrast, there is extensive literature showing the evaluation of turbulence models to predict indoor air conditions in single cavities or rooms with different convection regimes. These studies cover a broad variety of turbulence models, from the simplest models, such as the zero-equation model (Zhai et al., 2007) to more complex models, such as Detached Eddy Simulation (DES) (Zhang and Chen 2007, Zhang et al., 2007). Two-eddy viscosity turbulence models, such as $k-\varepsilon$ and $k-\omega$, are the most widely evaluated models for single enclosed cavities (Zhang et al., 2007; Posner et al., 2003; Choi et al., 2004; Rundle and Lightstone, 2007; Susin et al., 2009; Cao et al., 2011; Choi and Kim, 2012). Based on an extensive literature review, Cortés et al. (2014) concluded that overall, the $k-\varepsilon$ and $k-\omega$ models demonstrate a good performance in predicting indoor airflow conditions. Nevertheless, the accuracy of these two-eddy viscosity models is closely associated with the convection regime (i.e., natural, forced or mixed).

The objective of this paper is to evaluate five two-eddy viscosity turbulence models ($k-\varepsilon$ standard, $k-\varepsilon$ RNG, $k-\varepsilon$ realizable, $k-\omega$ standard and $k-\omega$ SST) in terms of predicting: i) the indoor air conditions in a full-scale, two-story test hut with heat and mass exchanged through an horizontal opening connecting two floors, and ii) the mass exchange rate across the horizontal opening. Therefore, this paper advances the evaluation of two-eddy viscosity turbulence models to predict indoor environmental conditions and interzonal mass exchanges for a scenario with two full-scale rooms connected via a horizontal opening representing a staircase.

The methodology used to evaluate the performance of five $k-\varepsilon$ and $k-\omega$ models via CFD simulations is based on the experimental results obtained by Vera et al. (2010a) and Vera (2009) in a full-scale, two-story test hut. The experimental results correspond to the indoor air conditions, such as temperature and air speed across the test hut, and the upward mass flow rates through the horizontal opening. The CFD simulation results for each turbulence model are compared with experimental results at different locations across the two-story test hut for each case of natural or mixed convection.



2. Full-scale two-story test hut experiment

The experimental setup considered in this paper is extensively described in Vera et al. (2010a), and therefore, this section briefly describes the main aspects of it. A two-story, full-scale test hut representing a typical wood-framed house was built inside the Environmental Chamber at Concordia University. This test-hut consisted of two rooms with internal dimensions of 3.62 m x 2.44 m x 2.43 m, each with a horizontal opening of 1.19 m x 0.91 m and 0.22 m thick. The opening connects the two rooms and allows for heat and airflow exchange. Figure 1a shows a schematic isometric view of the test hut. A baseboard heater was located at the bottom portion of the north wall in each room to provide the desired indoor temperature by varying the mean heating power. A moisture and heat source, which is labeled as the heat source in Figure 1a, is placed in the lower room and produces moisture at a constant rate.

The experimental average temperature difference between the lower and upper rooms, ΔT , was at most 3.5°C. Three ventilation strategies were studied as shown in Figure 2: no ventilation (scenario I), ventilation with a downward net flow through the opening (scenarios II) and independent ventilation in each room (scenario IV). These ventilation strategies correspond to natural convection (NC, scenario I) or mixed convection (MC, scenarios II and IV). The air speed across the two-story full-scale test hut was measured by 19 omnidirectional anemometers (hot-sphere type, model HT-412 probes and HT-428 transducers from Sensor Electronic and Measurement Equipment, Poland), while the indoor temperature and relative humidity were monitored by 64 sensors (Vaisala Humitter 50Y and HMP50). All sensors are distributed along the test hut at different heights and formed lines from the floor of the lower room to the ceiling of the upper room. For instance, Figure 1b shows the location of the temperature and relative humidity sensors in the lower room.

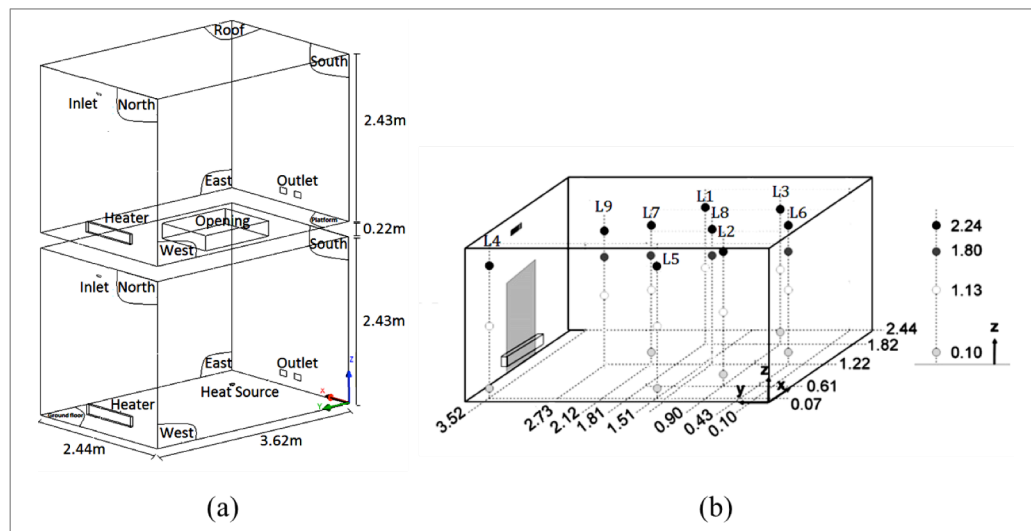


Figure 1. a) Schematic representation of the two-story test-hut, (b) distribution of temperature and relative humidity sensors in the lower room (dimension in meters)

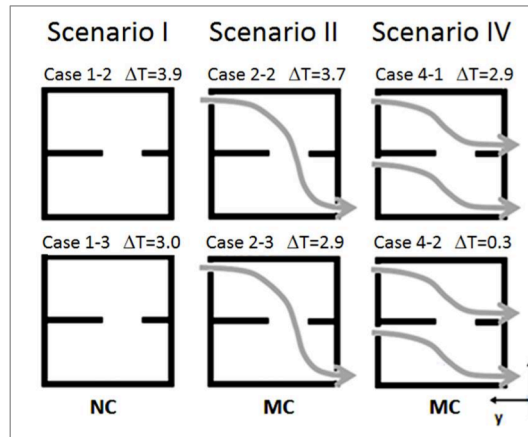


Figure 2. Ventilation scenarios tested: no ventilation (scenario I), single ventilation with downward net flow through the opening (scenarios II), and independent ventilation in each room (scenario IV)

3. CFD model

A CFD model of the full-scale two-story test hut was developed to simulate the indoor environmental conditions (i.e., temperature, moisture content, air speed) using a commercial CFD software package, Ansys Fluent v.14.0 (Ansys 2011). The indoor air condition quantities are governed by the conservation laws of mass, momentum and energy. Five two-eddy viscosity turbulence models were evaluated in this study. The models were the $k-\epsilon$ standard (Launder and Spalding, 1974), $k-\epsilon$ RNG (Yarkhot and Orszag, 1986), $k-\epsilon$ realizable (Shih et al., 1995), $k-\omega$ standard (Wilcox, 1988) and $k-\omega$ SST (Menter, 1994) models. The $k-\epsilon$ models are the most common ones for indoor airflow simulations due to their robust performance, whereas the $k-\omega$ models present a newer formulation for the near wall treatment. This formulation might make them more accurate and robust for indoor environmental conditions. These models were chosen due to their accuracy in the assessment of indoor environmental conditions, and they have been widely validated for single-zone indoor environments (Zhang and Chen, 2007; Zhang et al., 2007; Posner et al. 2003; Choi et al., 2004; Rundle and Lightstone, 2007; Susin et al. 2009; Zitzmann et al., 2005; Voigt, 2000; Rohdin and Moshfegh, 2011; Stamou and Katsiris, 2006; Moureh and Flick, 2003).

3.1 Geometry

The full-scale, two-story test hut was modeled in Ansys Fluent v.14. Walls were considered to be adiabatic with zero-thickness. The experimental surface temperatures at different locations for each case were set as the boundary conditions. The heat source was considered as a small cylinder with a sensible heat of 85 W. The ventilation inlets and outlets were rectangular sections of 96.5 mm wide by 21.8 mm high and 135.0 mm wide by 85.0 mm high, respectively. The baseboard heaters were modeled as rectangular objects of 0.045 m by 0.150 m by 0.920 m.

3.2 Numerical solution method

To predict the main indoor air conditions across the test-hut (i.e., temperatures, air speeds, airflow pattern) and

the interzonal mass airflow rate through the horizontal openings, 3-dimensional and steady-state simulations were performed in Ansys Fluent v.14. A second-order upwind differencing scheme was chosen to achieve a higher accuracy in the solutions. A Boussinesq approximation was considered, and therefore, the density was taken into account as a constant value in all solved equations, except for the buoyancy term. The convergence criteria were 10^{-6} for energy and 10^{-3} for the other variables. To obtain convergence, the under-relaxation factors were set between 0.15 and 0.5 for momentum; between 0.5 and 0.85 for pressure; to 1.0 for density, body forces, turbulent viscosity and energy; and to 0.8 for turbulent kinetic energy and turbulent dissipation rate. The Semi-Implicit Method for Pressure-Linked Equations (SIMPLE) was chosen as a default pressure-velocity coupling algorithm.

3.3 Grid verification

A hexahedral unstructured mesh (Figure 3a) was built with finer cells near the walls, inlet, outlets, baseboard heater and heat source to ensure a proper transfer of the boundary conditions to the air domain. A grid verification is needed to evaluate whether the CFD results are independent of the mesh. A mesh verification is usually performed by means of comparing the CFD results among the tested meshes with the experimental results. In this study, three different meshes were tested: $\Delta 1$, $\Delta 2$ and $\Delta 3$, as shown in Table 2. The finest mesh is $\Delta 1$, and $\Delta 3$ is the coarsest mesh. For case 2-3, Figure 3b shows, for example, the simulated and experimental results of the air temperature for these three meshes at lines 1, 8 and 9, as indicated in Figure 1b. The simulation results of the coarsest ($\Delta 3$) and medium ($\Delta 2$) mesh are very close to each other and in excellent agreement with experimental data, while the results of the finest mesh ($\Delta 1$) are not as accurate as the results for the other meshes.

The previous qualitative analysis does not allow for concluding which mesh has a good balance between accuracy and computational time. Therefore, a quantitative analysis is needed to verify that the grid independency is performed based on the quantification of the uncertainty of the grid convergence. This is performed by estimating the grid convergence index (GCI) (Roache, 1994; Hajdukiewicz et al., 2013). This index can be seen as the



ENGLISH VERSION.....

error estimator associated with the grid resolution and indicates how much the solution would change with a further refinement of the grid. The GCI is defined as

$$GCI^{fine} = Fs \frac{\varepsilon}{r^{p-1}} \quad (1)$$

$$p = \frac{\ln \left| \frac{f_{coarse} - f_{medium}}{f_{medium} - f_{fine}} \right|}{\ln r} \quad (2)$$

$$\varepsilon = \frac{f_{coarse} - f_{fine}}{f_{fine}} \quad (3)$$

$$r = \left(\frac{\Delta_{fine}}{\Delta_{coarse}} \right)^{1/3} \quad (4)$$

where Fs is the safety factor equal to 1.25 when comparing three grids Roache, 1994; p is the order of convergence, which has been calculated as the average p value over the sensors at the nine lines presented in Figure 1b, and is equal to 5.1; ε is the relative error between the coarse (f_{coarse}) and fine (f_{fine}) grid solutions; r is the refinement ratio between the number of grid elements of the fine and coarse 3D meshes. Therefore, GCI_{21} corresponds to the grid convergence error due to the refinement from mesh $\Delta 2$ (medium size) to mesh $\Delta 1$ (the finest mesh). Similarly, GCI_{32} is defined as the grid convergence error due to passing from the coarsest mesh $\Delta 3$ to the medium mesh $\Delta 2$.

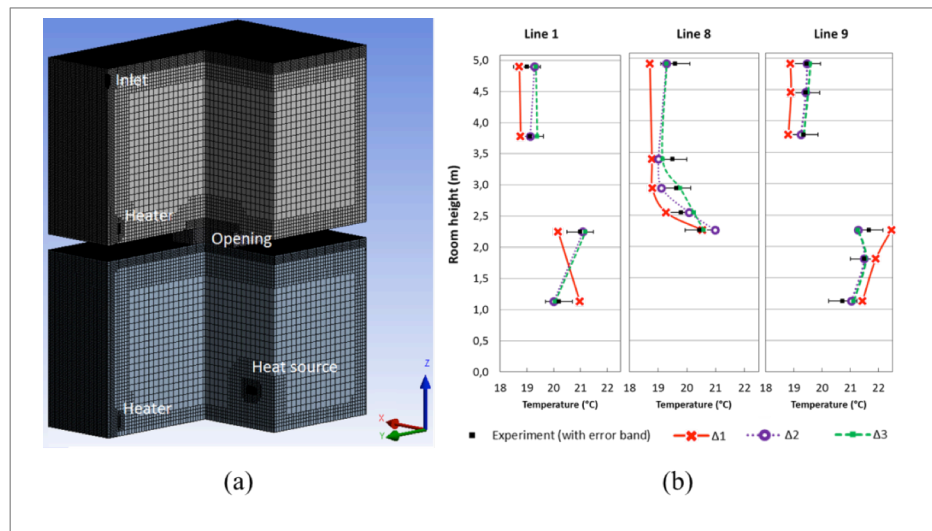


Figure 3. a) Computational mesh grid used. b) Predicted vertical temperatures at various points along vertical lines at different locations of the test-hut for three mesh sizes for case 2-3

Table 1. Experimental conditions for cases simulated Vera (2009)

Parameters	Case 1-2	Case 1-3	Case 2-2	Case 2-3	Case 4-1	Case 4-2
Supply air condition:						
Inlet airflow rate 1 (l/s)	-	-	5.929	5.905	3.290	3.295
Inlet Temperature 1 (°C)	-	-	18.00	18.00	17.81	18.20
Inlet airflow rate 2 (l/s)	-	-	-	-	2.951	2.880
Inlet Temperature 2 (°C)	-	-	-	-	18.01	17.90
Baseboard heater 1 (W)	230	290	274	252	175	143
Baseboard heater 2 (W)	-	170	-	91	90	166
Heat source, hotplate (W)	85	85	85	85	85	85
Wall surface temperatures lower room (°C)						
North wall	19.9	22.6	20.5	20.3	20.1	20.0
East wall	18.9	21.2	18.8	18.8	18.8	18.8
South wall	18.3	20.7	18.4	18.6	18.3	18.3
West wall	18.6	21.0	18.7	18.7	18.6	18.7
Ground floor	18.0	19.1	18.1	18.2	17.9	17.9
Ceiling	20.9	23.6	21.2	21.1	20.9	20.8
Wall surface temperatures upper room (°C)						
North wall	17.6	20.1	16.6	16.5	17.8	19.2
East wall	16.9	19.4	16.2	17.2	17.2	18.4
South wall	16.6	18.7	15.6	16.7	16.4	17.6
West wall	16.9	19.4	16.2	17.3	17.2	18.4
Floor	18.6	19.8	16.9	17.8	17.6	18.6
Ceiling	17.6	20.4	16.8	18.0	17.9	19.6

Table 2. Grid elements and refinement ratio for three different mesh sizes

$\Delta 1$	$\Delta 2$	$\Delta 3$	r32	r21
1,065,895	493,575	153,769	1.48	1.29

Table 3. Grid convergence index for indoor temperatures for three mesh sizes

z (m)	Experiment (°C)	$\Delta 1$	$\Delta 2$	$\Delta 3$	e32	e21	GCI_{32} (%)	GCI_{21} (%)
Line 1								
1.13	20.20	20.98	20.00	20.06	0.003	-0.047	0.056	-2.159
2.245	20.99	20.17	21.10	21.19	0.004	0.046	0.088	2.137
3.78	19.11	18.77	19.12	19.39	0.014	0.019	0.276	0.879
4.895	19.00	18.72	19.28	19.34	0.003	0.030	0.057	1.388
Line 8								
2.26	20.44	20.54	20.98	20.58	-0.019	0.022	-0.377	1.001
2.54	19.80	19.27	20.08	20.24	0.008	0.042	0.162	1.930
2.929	19.63	18.79	19.12	19.76	0.034	0.017	0.675	0.800
3.387	19.50	18.78	19.01	19.15	0.007	0.012	0.149	0.569
4.91	19.59	18.71	19.29	19.29	0.000	0.031	0.007	1.428
Line 9								
1.13	20.73	20.88	21.04	21.13	0.004	0.008	0.082	0.351
1.8	21.50	21.90	21.50	21.55	0.002	-0.018	0.048	-0.853
2.26	21.66	21.46	22.29	22.28	-0.001	0.039	-0.011	1.788
3.78	19.35	18.81	19.25	19.35	0.005	0.024	0.105	1.094
4.45	19.42	18.90	19.42	19.50	0.004	0.028	0.077	1.295
4.91	19.45	18.88	19.47	19.59	0.006	0.031	0.122	1.452



The GCI indices are shown in Table 3 for the air temperature data at several locations of lines 1, 8 and 9, as indicated in Figure 1b. The largest GCIs are obtained when refining from mesh $\Delta 2$ to $\Delta 1$, and these GCIs are close to the accuracy of temperature measurements (2%), whereas the GCIs for refining mesh $\Delta 3$ to $\Delta 2$ are much smaller for all measurement points. This means that all meshes can be used for further analysis. Nevertheless, mesh $\Delta 1$, which has 1,065,895 elements, would have a higher computational cost than meshes $\Delta 2$ and $\Delta 3$ without achieving more accurate results. The convergence error is much smaller when the mesh is refined from the coarsest to the medium mesh. This suggests that mesh $\Delta 2$, which has 493,575 elements, has a good balance between accuracy and computing time.

4. General CFD results

The CFD model of the full-scale, two-story test hut predicts three main parameters of the indoor environment: temperature distributions, air speed distributions and airflow pattern. Due to the length limitation of this paper, the airflow pattern and temperature distribution across the longitudinal axis of the two-story test hut are only shown for case 2-3 (Figure 4). The flow is significantly influenced by strong buoyancy air currents rising from the baseboard heaters and heat/moisture source. Temperature stratification is observed in the lower room, while temperature is more

uniform in the upper room. Additionally, it is shown that a two-way airflow exists across the opening and that the heat and mass exchange through the opening is highly affected by the warm air currents. Similar general results are found for other natural and mixed convection cases, as seen in Cortés (2013).

5. Evaluation of turbulence models

5.1 Evaluation of the turbulence models to predict the indoor temperature and air speed distributions

This section evaluates five two-eddy viscosity turbulence models in terms of their capability to predict indoor air conditions (i.e., temperature and air speed) under the scenario in which heat and mass exchange occurs through a horizontal opening that connects two floors. The evaluated turbulence models are the $k-\epsilon$ standard, $k-\epsilon$ RNG, $k-\epsilon$ realizable, $k-\omega$ standard and $k-\omega$ SST models. Although these turbulence models have been extensively evaluated to predict indoor air quantities in single rooms and cavities, they have not been evaluated under the scenario described above.

In this study, the testing of the turbulence models for six different cases dominated either by natural or mixed convection is performed. The experimental data required to carry out the evaluation were reported by Vera (2009). The main boundary conditions for each case are summarized in Table 1. A CFD model for each case was built according to the procedure shown in section 3.

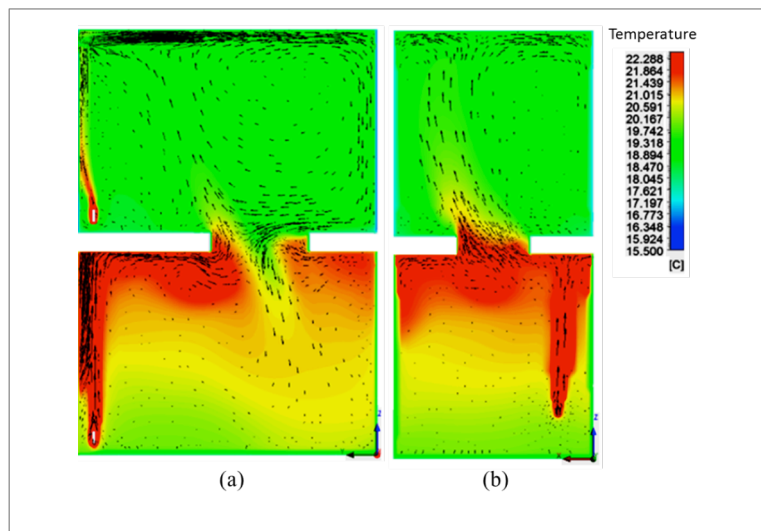


Figure 4. Visualization of warm convective currents for Case 2-3 (MC) at cross section: a) $x = 1.22$ m, b) $y = 1.81$ m

The evaluation of the five two-eddy viscosity models was carried out, first, by qualitatively comparing the experimental and CFD simulation results for the air temperatures and speeds at specific locations (i.e., the lines shown in Figure 1b). This qualitative analysis provides evidence about the capability of the turbulence models to predict the air temperatures and speeds as well as their profiles along the test-hut height at different locations. Although the simulated data from all turbulence models are in good agreement with the experimental values, each data point is best predicted by different turbulence models, which makes it difficult to establish which turbulence model has the best overall performance. Therefore, the quantitative evaluations were carried out based on the normalized root-mean-square error (RMSE). The following sections present these results and evaluations. Due to the length limitation of the paper, only results for three cases (i.e., 1-2, 2-3 and 4-1) are shown below.

5.1.1 Qualitative evaluation

The predicted indoor temperatures and air speeds by the five $k-\varepsilon$ and $k-\omega$ turbulence models are compared with experimental data of Vera (2009) in Figures 5, 6 and 7 for cases 1-2, 2-3 and 4-1, respectively.

These figures show that all turbulence models can predict well the pattern of the temperature along the test-hut height for different lines. A temperature stratification of 2°C-3°C exists in the lower room. On the other hand, the temperature distribution is rather uniform across the upper room. The results show an excellent agreement between the simulated temperatures in the upper room and experimental data for all five evaluated turbulence models, while differences of up to 1°C can be observed between the simulated and experimental data in the lower room for some of the turbulence models. In addition, the simulated temperatures in some locations on lines 8 and 9 for case 1-2 are underpredicted by 2°C. There is no clarity about the causes of these significant temperature differences in these two locations.

Figures 5, 6 and 7 also show that all turbulence models are able to reasonably predict the air speed profile along lines 8 and 9. However, the results show larger variations of the forecasted air speeds among the turbulence models. Differences with the experimental data for the predicted temperatures and air speeds among the turbulence models emphasize the need for evaluating their performance to estimate the interzonal heat and mass exchange through horizontal openings in buildings.

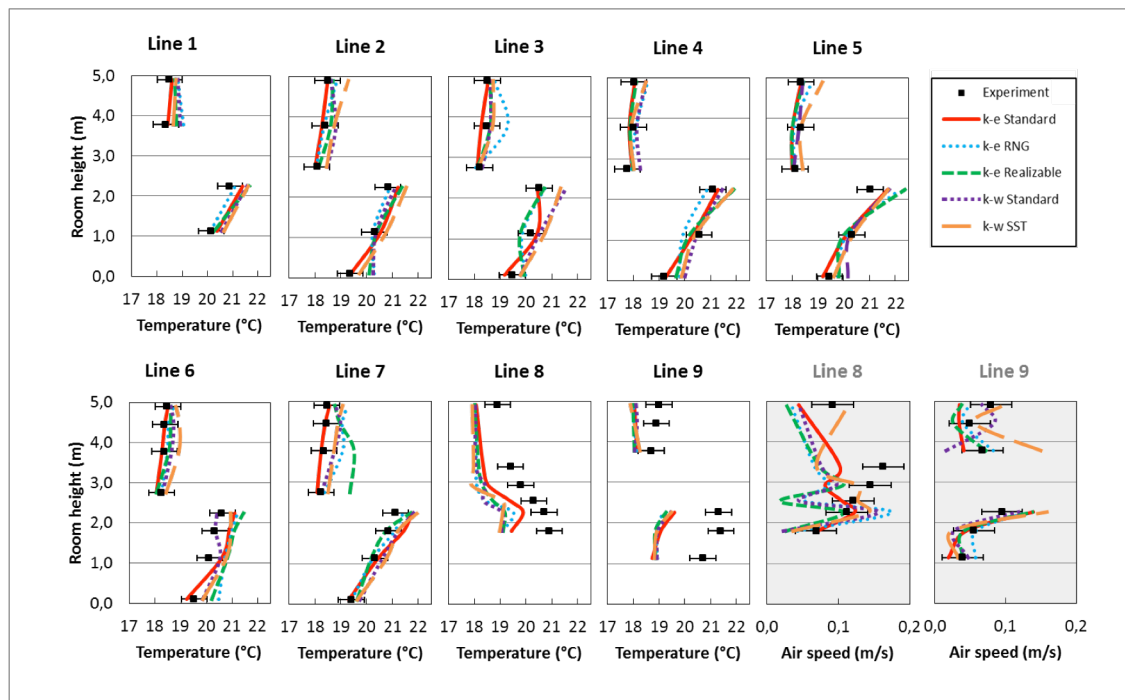


Figure 5. Comparison of the simulated and measured temperatures and air speeds for case 1-2



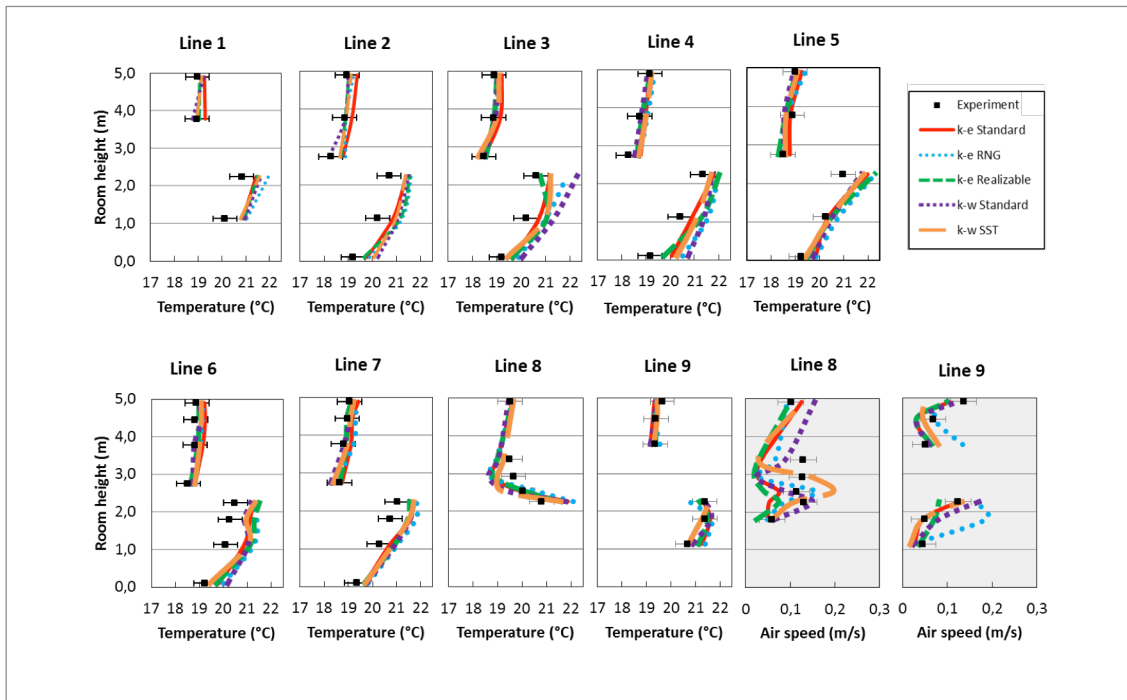


Figure 6. Comparison of the simulated and measured temperatures and air speeds for case 2-3

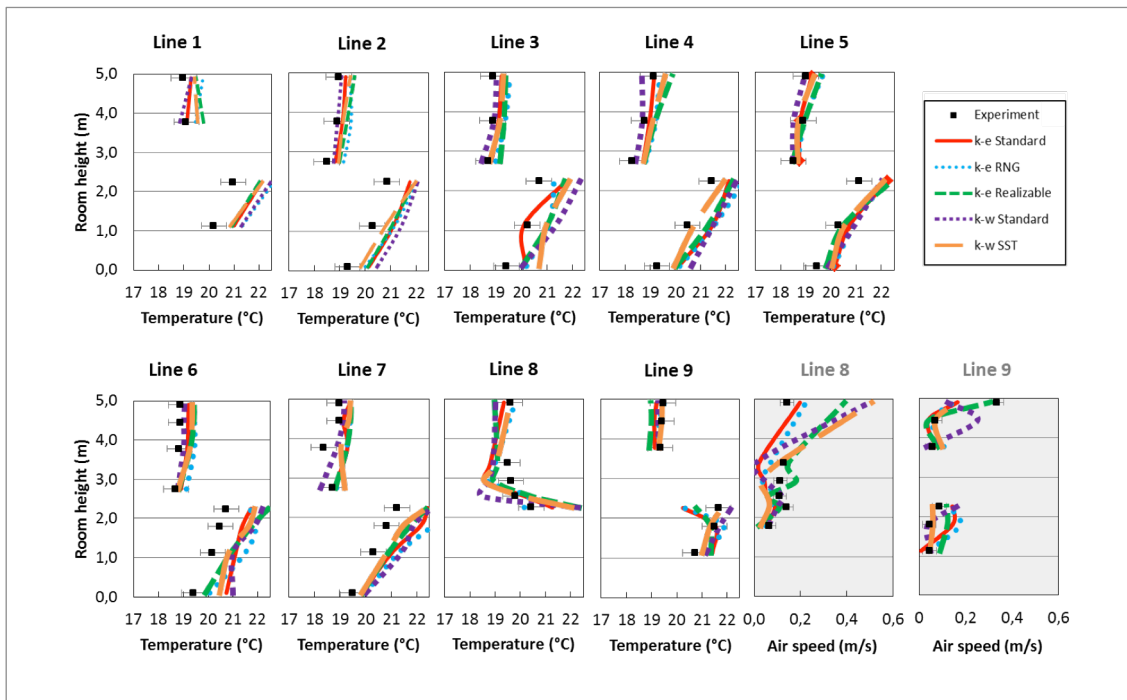


Figure 7. Comparison of the simulated and measured temperatures and air speeds for case 4-1



5.1.2 Quantitative evaluation

Because one model may provide a better simulated quantity at one location but worse one at another, it is necessary to establish the overall performance of each model quantitatively. The normalized RMSE index is applied based on the procedure described by Wang and Zhai (2012). The RMSE is used to evaluate how far the prediction deviates from the experimental data by considering first the experimental measurement uncertainty and then normalizing the deviation by the absolute value of the measured data. The RMSE is defined as

$$RMSE(P, M) = \sqrt{\frac{\sum_{i=1}^n \delta_{pm} (|P(i)-M(i)|-e(i))^2}{\sum_{i=1}^n M(i)^2}} \quad (5)$$

$$\delta_{pm} = \begin{cases} 1 & |P(i)-M(i)| > e(i) \\ 0 & |P(i)-M(i)| < e(i) \end{cases} \quad (6)$$

where $P(i)$ and $M(i)$ are the prediction and measurement datasets at certain locations, respectively, and $e(i)$ is the experimental measurement uncertainty. The RMSE was calculated for all locations with the available experimental data. Therefore, the index was calculated with 56 data points for the temperature distribution and 12 data points for the air speed distribution. Then, the RMSE for the cases of each convection type was averaged to obtain a

unique RMSE value for each turbulence model and convection type. Tables 4 and 5 show the RMSE indices for the temperatures and air speeds for the natural convection cases (i.e., cases 1-2 and 1-3) and mixed convection cases (i.e., cases 2-2, 2-3, 4-1 and 4-2), respectively.

The results show that the $k-\epsilon$ standard model has the lowest deviations between the experimental data and the predicted air temperature and speed for the natural convection cases (Table 4). The average RMSE indices are 0.019 for temperature and 0.134 for air speed. For the mixed convection cases, the $k-\epsilon$ realizable model reveals the lowest RMSE indices to be 0.014 and 0.429 for temperature and air speed, respectively (Table 5). This means that the $k-\epsilon$ standard and the $k-\epsilon$ realizable models have shown the best overall performance among the two-eddy viscosity turbulence models evaluated in this paper for natural and mixed convection, respectively.

Despite that a specific turbulence model shows better performance for each characteristic convection flow, all turbulence models possess a similar magnitude of RMSE for the temperature in both the natural and mixed convection cases. Therefore, the five evaluated two-eddy viscosity models perform well when predicting temperature. However, the larger values of the RMSE for air speed and the differences among the turbulence models suggest that the air speed is not predicted by all turbulence models with the same accuracy.

Table 4. RMSE index for natural convection cases

Temperature RMSE						Velocity RMSE					
Case	k-ε standard	k-ε RNG	k-ε realizable	k-ω standard	k-ω SST	Caso	k-ε standard	k-ε RNG	k-ε realizable	k-ω standard	k-ω SST
1-2	0.031	0.034	0.035	0.032	0.033	1-2	0.221	0.319	0.407	0.292	0.234
1-3	0.006	0.005	0.008	0.010	0.006	1-3	0.047	0.320	0.193	0.241	0.277
Average	0.019	0.0200	0.022	0.021	0.020	Promedio	0.134	0.319	0.30	0.267	0.256



Table 5. RMSE index for mixed convection cases

Temperature RMSE						Velocity RMSE					
Case	k-ε standard	k-ε RNG	k-ε realizable	k-ω standard	k-ω SST	Case	k-ε standard	k-ε RNG	k-ε realizable	k-ω standard	k-ω SST
2-2	0.021	0.018	0.010	0.019	0.020	2-2	0.514	0.282	0.501	0.423	0.631
2-3	0.016	0.021	0.018	0.024	0.015	2-3	0.520	0.525	0.383	0.676	0.651
4-1	0.008	0.016	0.011	0.015	0.009	4-1	0.520	0.525	0.383	0.676	0.651
4-2	0.022	0.024	0.018	0.017	0.018	4-2	0.432	0.388	0.448	0.337	0.251
Average	0.017	0.020	0.014	0.019	0.016	Average	0.497	0.430	0.429	0.528	0.540

5.2 Evaluation of turbulence models’ ability to predict the mass airflow through the horizontal opening

The previous section has shown the capability of five two-eddy turbulence models to predict the indoor air conditions in a scenario where the interzonal heat and mass exchanges across a horizontal opening that connects two floors. Additionally, this section evaluated the ability of the turbulence models to predict the upward mass airflows through the horizontal opening for those that showed the best performance in section 5.1, the k-ε standard model for the natural convection cases and the k-ε realizable for the mixed convection cases. The experimental data of Vera (2009) was used to perform this evaluation.

The total upward mass airflow, ma_{up} , through the opening can be calculated from simulated results as the sum of the mass airflow in each cell, ma_i , in the middle plane of the opening ($z = 2.54$ m) as follows:

$$ma_i(kg/s) = A_i * \rho_i * V_{zi} \tag{6}$$

$$ma_{up}(kg/s) = \sum_1^N ma_i ; \text{ if } ma_i > 0 \tag{7}$$

$$ma_{down}(kg/s) = \sum_1^N ma_i ; \text{ if } ma_i < 0 \tag{8}$$

where $A_i = A/N$. A is the horizontal opening area (m^2) and N is the number of cells in the middle plane. Because the mesh grid in the opening (i.e., plane XY) is uniform, the area of each cell is equal to A_i . The vertical component of the air velocity in each cell is V_{zi} , and ρ_i is the air density as defined by Equation 9, where T_i is the temperature in each cell of the opening in Kelvin.

$$\rho_i(kg/m^3) = \frac{101.325}{287.055 * T_i} \tag{9}$$

Figure 8 shows the measured and simulated upward mass airflow rates for all cases studied. The k-ε realizable model predicts the mass airflow through the opening with excellent agreement with measured data for the mixed convection cases. The predicted upward mass airflows are within the uncertainty of the experimental measurements. The highest difference is found in case 4-2, which has a percent error of 8.5%, and the lowest difference is for case 2-2, which has a percent error of 1.3%.

Otherwise, the results of the k-ε standard model for the natural convection (NC) cases are not as good as the results found for the mixed convection (MC) cases. In particular, the predicted mass airflow rate for case 1-2 (37.08×10^{-3} kg/s) is much lower than the measured value ($61.00 \times 10^{-3} \pm 16.5 \times 10^{-3}$ kg/s). This result might show the difficulty in predicting the mass airflow through horizontal openings when the buoyancy forces dominate the mass exchange. Although the airflow through a horizontal opening has not been extensively studied, the available literature shows that the airflow pattern is highly unstable for natural convection. Therefore, it is expected that this phenomenon would be difficult to predict.



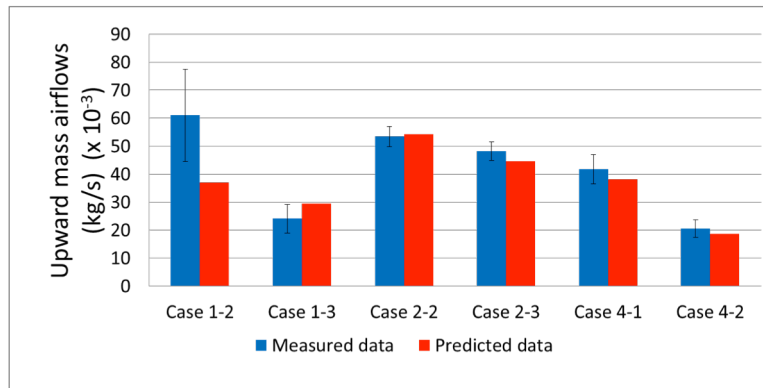


Figure 8. Measured and simulated upward mass airflow rates through the opening for all studied cases

6. Conclusions

Interior building openings, such as stairwell openings, are important paths for the exchange of heat, air, moisture and pollutants. However, the interzonal airflow through horizontal openings has not been studied in depth. Moreover, there is limited information about the performance of turbulence models to predict the indoor air conditions and vertical interzonal exchanges under this scenario for natural and mixed convection.

This paper focused on the evaluation of five two-eddy viscosity turbulence models (the $k-\epsilon$ standard, $k-\epsilon$ RNG, $k-\epsilon$ realizable, $k-\omega$ standard and $k-\omega$ SST) in terms of predicting: i) the indoor air conditions in a full-scale, two-story test hut with heat and mass exchanged through an horizontal opening connecting the two floors, and ii) the mass exchange rate across the horizontal opening for cases of natural and mixed convection. This evaluation was performed by comparing the simulated CFD results with the experimental data of Vera (2009) at different locations. The main conclusions from this study are as follows:

- Based on the RMSE index, the $k-\epsilon$ standard and $k-\epsilon$ realizable models are the most accurate turbulence models to predict the temperature and air speed distributions across a full-scale, two-story test hut for the natural and mixed convection cases, respectively.
- The low values of the RMSE indices for the temperature indicate that all five of the $k-\epsilon$ and $k-\omega$ turbulence models evaluated predict the temperature distribution with good agreement with the experimental data for both the natural and mixed convection cases. However, the qualitative analysis shows that the turbulence models evaluated underpredict the air temperature by up to 2°C in some locations on lines 8 and 9 for the natural convection cases.
- For the air speed, all of the turbulence models provide reasonable predictions along lines 8 and 9. However, significant differences for some of the simulated results are found among the turbulence models. This fact is also reflected by a larger variation and higher RMSE indices for the air

speed, as shown in Tables 4 and 5. For the natural convection case, the RMSE indices for the air speed lie between 0.13 and 0.3, while for mixed convection cases, they are between 0.42 and 0.54.

- The $k-\epsilon$ standard and $k-\epsilon$ realizable models show excellent performance for predicting the interzonal mass airflows through the horizontal opening for the natural and mixed convection cases, respectively.

This paper advances the evaluation of two-eddy viscosity turbulence models to predict indoor environmental conditions and interzonal mass exchanges for the scenario of two full-scale rooms connected via a horizontal opening, which represents a staircase opening. The $k-\epsilon$ standard and $k-\epsilon$ realizable turbulence models have shown the best performance, and therefore, they should be used for improved CFD simulations of multi-zone buildings at the design stage to achieve more comfortable and healthy indoor environments.

In subsequent work, these two turbulence models are used to study the effect of the opening aspect ratio (width/length) on the heat and mass transfer through horizontal openings for natural and mixed convection cases.

7. Acknowledgements

This work was funded by the National Commission for Scientific and Technological Research of Chile (CONICYT) under the research grant FONDECYT 11100120. Additionally, this work was supported by the research project CONICYT/FONDAP 15110020. Some aspects of this work were developed during a stay at Magdalena Cortés at Concordia University (Montreal, Canada), which was funded by the Canada-Chile Leadership Exchange Scholarship. The authors would also like to acknowledge the paper's preliminary comments of Dr. Leon Wang from Concordia University.



8. References

- ANSYS (2011)**, ANSYS FLUENT Theory Guide: Release 14, in, ANSYS.
- Blomqvist C. and Sandberg M. (2004)**, Air movements through horizontal openings in buildings - A model study, *The International Journal of Ventilation*, 3(1) 1-10.
- Brown W.G. (1962)**, Natural convection through rectangular openings in partitions—2: Horizontal partitions, *International Journal of Heat and Mass Transfer*, 5(9) 869-881.
- Cao G., Ruponen M., Paavilainen R. and Kurnitski J. (2011)**, Modelling and simulation of the near-wall velocity of a turbulent ceiling attached plane jet after its impingement with the corner, *Building and Environment*, 46(2) 489-500.
- Cortés M. (2013)**, Natural and mixed convective heat transfer through horizontal openings in buildings, M.Sc. Thesis, Department of Construction Engineering and Management, Pontificia Universidad Católica de Chile, Santiago.
- Cortés M., Fazio P., Rao J., Bustamante W. and Vera S. (2014)**, CFD modeling of basic convection cases in enclosed environments: Needs of CFD beginners to acquire skills and confidence on CFD modeling, *Revista de Ingeniería de Construcción (RIC)*, 29(1) 22-45.
- Cooper L.Y. (1995)**, Combined Buoyancy and Pressure-Driven Flow Through a Shallow, Horizontal, Circular Vent, *Journal of Heat Transfer*, 117(3) 659-667.
- Chen Q. and Xu W. (1998)**, A zero-equation turbulence model for indoor airflow simulation, *Energy and Buildings*, 28(2) 137-144.
- Choi S.-K., Kim E.-K., Wi M.-H. and Kim S.-O. (2004)**, Computation of a turbulent natural convection in a rectangular cavity with the low-reynolds-number differential stress and flux model, *KSME International Journal*, 18(10) 1782-1798.
- Choi S.-K., Kim S.-O. (2012)**, Turbulence modeling of natural convection in enclosures: A review, *J Mech Sci Technol*, 26(1) 283-297.
- Epstein M. (1988)**, Buoyancy-driven exchange flow through small openings in horizontal partitions, *Journal of Heat Transfer*, 110(4) 885-893.
- Hajdukiewicz M., Geron M. and Keane M.M. (2013)**, Formal calibration methodology for CFD models of naturally ventilated indoor environments, *Building and Environment*, 59(0) 290-302.
- Heiselberg P. and Li Z. (2009)**, Buoyancy driven natural ventilation through horizontal openings, *The International Journal of Ventilation*, 8(3) 219-231.
- Klobut K. and Sirén K. (1995)**, Air flows measured in large openings in a horizontal partition, *Building and Environment*, 29(3) (1994) 325-335.
- Lauder B.E. and Spalding D.B. (1974)**, The numerical computation of turbulent flows, *Computer Methods in Applied Mechanics and Engineering*, 3(2) 269-289.
- Li Z. (2007)**, Characteristics of Buoyancy Driven Natural Ventilation through Horizontal Openings, Ph.D. Thesis defended public at Aalborg University (101106), Aalborg University, Aalborg.
- Menter F.R. (1994)**, 2-equation eddy-viscosity turbulence models for engineering applications, *Aiaa J.*, 32(8) 1598-1605.
- Moureh J. and Flick D. (2003)**, Wall air-jet characteristics and airflow patterns within a slot ventilated enclosure, *International Journal of Thermal Sciences*, 42(7) 703-711.
- Peppes A.A., Santamouris M. and Asimakopoulos D.N. (2001)**, Buoyancy-driven flow through a stairwell, *Building and Environment*, 36(2) 167-180.
- Peppes A.A., Santamouris M. and Asimakopoulos D.N. (2002)**, Experimental and numerical study of buoyancy-driven stairwell flow in a three storey building, *Building and Environment*, 37(5) 497-506.
- Posner J.D., Buchanan C.R., Dunn-Rankin D. (2003)**, Measurement and prediction of indoor air flow in a model room, *Energy and Buildings*, 35(5) 515-526.
- Riffat S.B. and Kohal J.S. (1994)**, Experimental study of interzonal natural convection through an aperture, *Applied Energy*, 48(4) 305-313.
- Riffat S.B., Kohal J.S. and Shao L. (1994)**, Measurement and CFD modeling of buoyancy-driven flows in horizontal openings, in: *IAQ'94: Engineering Indoor Environments*, American Society of Heating, Refrigerating and Air-Conditioning Engineers, Inc., pp. 159-166.
- Riffat S.B. and Shao L. (1995)**, Characteristics of buoyancy-driven interzonal airflow via horizontal openings, *Building Services Engineering Research and Technology*, 16(3) 149-152.
- Roache P.J. (1994)**, Perspective: A Method for Uniform Reporting of Grid Refinement Studies, *Journal of Fluids Engineering*, 116(3) 405-413.
- Rohdin P. and Moshfegh B. (2011)**, Numerical modelling of industrial indoor environments: A comparison between different turbulence models and supply systems supported by field measurements, *Building and Environment*, 46(11) 2365-2374.
- Rundle C.A., Lightstone M.F. (2007)**, Validation of turbulent natural convection in square cavity for application of CFD modelling to heat transfer and fluid flow in atria geometries, in: *2nd Canadian Solar Building Conference*, Calgary, Canada, pp. 8.
- Shih T.-H., Liou W.W., Shabbir A., Yang Z. and Zhu J. (1995)**, A new $k-\epsilon$ eddy viscosity model for high reynolds number turbulent flows, *Computers & Fluids*, 24(3) 227-238.
- Stamou A. and Katsiris I. (2006)**, Verification of a CFD model for indoor airflow and heat transfer, *Building and Environment*, 41(9) 1171-1181.
- Susin R.M., Lindner G.A., Mariani V.C., Mendonça K.C. (2009)**, Evaluating the influence of the width of inlet slot on the prediction of indoor airflow: Comparison with experimental data, *Building and Environment*, 44(5) 971-986.
- Tan Q. and Jaluria Y. (2001)**, Mass flow through a horizontal vent in an enclosure due to pressure and density differences, *International Journal of Heat and Mass Transfer*, 44(8) 1543-1553.
- Vera S. (2009)**, Interzonal air and moisture transport through large horizontal openings: An integrated experimental and numerical study. Ph.D. Thesis, Concordia University, Montreal, Canada.
- Vera S., Rao J., Fazio P. and Campo A. (2014)**, Mixed convective heat transfer through a horizontal opening in a full-scale, two-story test-hut, *Applied Thermal Engineering*, 64(1-2) 499-507.
- Vera S., Fazio P. and Rao J. (2010a)**, Interzonal air and moisture transport through large horizontal openings in a full-scale two-story test-hut: Part 1 – Experimental study, *Building and Environment*, 45(5) 1192-1201.
- Vera S., Fazio P. and Rao J. (2010b)**, Interzonal air and moisture transport through large horizontal openings in a full-scale two-story test-hut: Part 2 – CFD study, *Building and Environment*, 45(3) 622-631.
- Voigt L.K. (2000)**, Comparison of Turbulence Models for Numerical Calculation of Airflow in an annex 20 Room, in, *International Centre for Indoor Environment and Energy*. Department of Energy Engineering. Technical University of Denmark.
- Wang H. and Zhai Z. (2012)**, Application of coarse-grid computational fluid dynamics on indoor environment modeling: Optimizing the trade-off between grid resolution and simulation accuracy, *HVAC&R Research*, 18(5) 915-933.
- Wilcox D.C. (1988)**, Reassessment of the scale-determining equation for advanced turbulence models, *Aiaa J.*, 26(11) 1299-1310.
- Yakhot V. and Orszag S.A. (1986)**, Renormalization-Group Analysis of Turbulence, *Physical Review Letters*, 57(14) 1722-1724.
- Zhai Z.J., Zhang Z., Zhang W. and Chen Q.Y. (2007)**, Evaluation of Various Turbulence Models in Predicting Airflow and Turbulence in Enclosed Environments by CFD: Part 1—Summary of Prevalent Turbulence Models, *HVAC&R Research*, 13(6) 853-870.
- Zhang T. and Chen Q. (2007)**, Novel air distribution systems for commercial aircraft cabins, *Building and Environment*, 42(4) 1675-1684.
- Zhang Z., Zhang W., Zhai Z.J. and Chen Q.Y. (2007)**, Evaluation of Various Turbulence Models in Predicting Airflow and Turbulence in Enclosed Environments by CFD: Part 2—Comparison with Experimental Data from Literature, *HVAC&R Research*, 13(6) 871-886.
- Zitzmann T., Cook M. and Pfrommer P. (2005)**, Simulation fo steady-state natural convection using CFD, in: *Building Simulation*, Montréal, Canada, pp. 1449-1456.

